

Self-compression pulse shaping by using non-degenerate two-photon absorption in silicon-on-insulator waveguides

J.-W. WU^{a*}, W.-H. ZHU^a, Y. XU^a, F.-G. LUO^b

^aInstitute of Optoelectronics Science & College of Science, Hohai University, Nanjing 210098, P.R. China

^bWuhan National Laboratory for Optoelectronics & College of Optoelectronics Science and Engineering, Huazhong University of Science and Technology, Wuhan 430074, P.R. China

To shape the self-compression signal pulse induced by free carrier absorption (FCA) in silicon-on-insulator (SOI) waveguides, in this letter a novel project is proposed and numerically simulated by co-propagating intensity pump pulse. Numerical results show that pulsewidth compression by up to a factor of ~ 3 can be achieved by adjusting the initial delay between pump and signal pulse. Furthermore, the properties of shaped pulse are strongly dependent on the parameters such as delay, energy and pulsewidth of pump pulse, and waveguide length.

(Received November 27, 2008; accepted January 21, 2009)

Keywords: Integrated optics, Silicon-on-insulator waveguides, Optical pulse compression and shaping, Non-linear absorptions

1. Introduction

Silicon photonics has attracted much attention recently and investigated extensively because of its potential applications in integrated optics and optoelectronics [1]. In particular, amongst the available material systems, the SOI waveguides with the high-index contrast have received tremendous interest due to the presence of strong nonlinear effects. Therefore, a wide range of optical devices has been realized on the SOI platform, including optical amplification and laser [2-4], optical switches [5], optical modulators [6], wavelength conversion [7], variable optical attenuators [8], optical add/drop filters [9], and pulse generation [10], and so on. Most of nonlinear devices are designed for steady state response, however, in pulse applications, the nonlinear transient behaviors of TPA and FCA have prominent effect on the final outcome, i.e., pulse will occur self-compression phenomenon due to FCA, and self-broadening because of TPA. As a consequence, the resultant pulse is distorted by the modulation of nonlinear processes. In this letter, we will focus only on the self-compression pulse shaping by co-propagating pump pulse with enough high energy based in the SOI waveguides. In fact, similar approach about pulse compression has already been thoroughly explored and investigated in semiconductor optical amplifiers [11]. In our modeling, the nonlinear coupled propagation equations are solved numerically to observe the dynamic properties of self-compression pulse shaping and compression. It is shown that the self-compression pulse can be compressed effectively by the influence of non-degenerate TPA that

will be performed when the self-compression pulse overlaps with the pump pulse along the SOI.

2. Modeling and equations

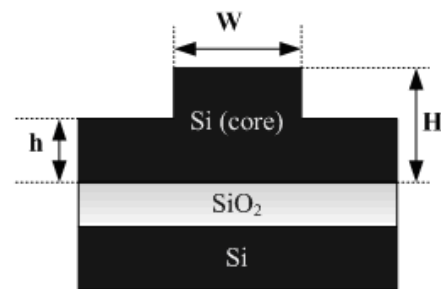


Fig. 1. The cross section of SOI waveguide.

The adopted SOI waveguide is presented in Fig. 1, whose cross section has the ridge structure.

In Fig. 1, the ridge waveguide structure with width W , rib height H , and slab height h . The free carriers will be produced when optical wave propagating in SOI waveguide, whose effective recombination lifetime τ_{eff} may be denoted by [12]

$$\tau_{eff}^{-1} = \frac{S}{H} + \frac{w + 2(H-h)}{wH} S' + 2 \frac{h}{H} \sqrt{\frac{D}{w^2} \left(\frac{S+S'}{h} \right)} \quad (1)$$

where the first term refers to the interface recombination lifetime, the second term refers to the surface recombination at the sidewalls, and last term refers to

transit time out of the modal area. S and S' are the effective surface recombination velocity, D is diffusion coefficient.

The nonlinear propagation equations of pump and signal pulses in SOI waveguide can be described by [13-16]

$$\begin{aligned} \frac{\partial A_p}{\partial z} + \beta_{p1} \frac{\partial A_p}{\partial t} + i \frac{1}{2} \beta_{p2} \frac{\partial^2 A_p}{\partial t^2} - \frac{1}{6} \beta_{p3} \frac{\partial^3 A_p}{\partial t^3} = & (2) \\ -\frac{1}{2} \alpha_{pl} A_p - \frac{1}{2} \alpha_{pFC} A_p - \frac{1}{2} \frac{\beta_{TPA}}{A_{p,eff}} |A_p|^2 A_p - \frac{\beta_{TPA}}{A_{p,eff}} |A_s|^2 A_p & \\ + i \gamma_{p,p} |A_p|^2 A_p + i 2 \gamma_{p,s} |A_s|^2 A_p + i \frac{2\pi}{\lambda_p} \Delta n_{\lambda_p} A_p & \end{aligned}$$

$$\begin{aligned} \frac{\partial A_s}{\partial z} + \beta_{s1} \frac{\partial A_s}{\partial t} + i \frac{1}{2} \beta_{s2} \frac{\partial^2 A_s}{\partial t^2} - \frac{1}{6} \beta_{s3} \frac{\partial^3 A_s}{\partial t^3} = & (3) \\ -\frac{1}{2} \alpha_{sl} A_s - \frac{1}{2} \alpha_{sFC} A_s - \frac{1}{2} \frac{\beta_{TPA}}{A_{s,eff}} |A_s|^2 A_s - \frac{\beta_{TPA}}{A_{s,eff}} |A_p|^2 A_s & \\ + i \gamma_{s,s} |A_s|^2 A_s + i 2 \gamma_{s,p} |A_p|^2 A_s + i \frac{2\pi}{\lambda_s} \Delta n_{\lambda_s} A_s & \end{aligned}$$

where the subscript p and s denote pump and signal pulses, respectively. A is the slowly varying pulse envelope, β_1, β_2 and β_3 are the first-, second-, and third-order dispersion coefficients. The parameter β_1 is related to the group velocity v_g of the pulse by $v_g = 1/\beta_1$, while β_2 governs the effect of group velocity dispersion, β_3 governs the effects of third-order dispersion and becomes important for ultrashort pulses because of their wide bandwidth. $\gamma = 2\pi n_2 / \lambda A_{eff}$ is the nonlinear parameter (n_2 is the nonlinear coefficient, c is the speed of light in free space, and A_{eff} is known as the effective core area, λ is the center wavelength of pulse.), α_l is the linear propagation loss. α_{FC} is the FCA coefficient. β_{TPA} is the TPA coefficient. The first four terms on the right-hand side of each equation denote the propagation loss, FCA loss, degenerate TPA and non-degenerate TPA, respectively. The next two terms represent the self-phase modulation and cross-phase modulation, respectively, and the final term describes free carrier dispersion that is related to efficient index change Δn that can be described by

$$\Delta n_{p,s} = -8.8 \times 10^{-22} \cdot \left(\frac{\lambda_{p,s}}{1.55} \right)^2 \Delta n_e - 8.5 \times 10^{-18} \cdot \left(\frac{\lambda_{p,s}}{1.55} \right)^2 (\Delta n_h)^{0.8} \quad (4)$$

and FCA coefficient is written as

$$\begin{aligned} \alpha_{FC} &= 8.5 \times 10^{-18} \cdot \left(\frac{\lambda_{p,s}}{1.55} \right)^2 \Delta n_e + 6.0 \times 10^{-18} \cdot \left(\frac{\lambda_{p,s}}{1.55} \right)^2 \Delta n_h \quad (5) \\ &= \sigma \cdot n \\ &= \sigma_0 \cdot \left(\frac{\lambda_{p,s}}{1.55} \right)^2 n \end{aligned}$$

where The coefficient $\sigma_0 = 1.45 \times 10^{-17} \text{ cm}^2$ is the free-carrier absorption cross section measured at $\lambda = 1.55 \mu\text{m}$. $n = n_e = n_h$ is the density of electron-hole pairs generated by the two-photon absorption process, and given by

$$\begin{aligned} \frac{dn}{dT} &= -\frac{n}{\tau_{eff}} + \frac{\beta_{TPA}}{2\hbar\omega_p} (|A_p(z, T)|^2 \cdot A_{p,eff}^{-1})^2 + \frac{\beta_{TPA}}{\hbar\omega_p} (|A_p(z, T)|^2 \cdot |A_s(z, T)|^2 \cdot A_{p,eff}^{-1})^2 \\ &+ \frac{\beta_{TPA}}{2\hbar\omega_s} (|A_s(z, T)|^2 \cdot A_{s,eff}^{-1})^2 + \frac{\beta_{TPA}}{\hbar\omega_s} (|A_s(z, T)|^2 \cdot |A_p(z, T)|^2 \cdot A_{s,eff}^{-1})^2 \end{aligned} \quad (6)$$

In some cases, if operation pulse has enough duration time, the terms of time relation may be neglected in Eqs. (2) and (3), and thus the partial differential equations can be transformed into ordinary differential equations by writing

$$\begin{aligned} \frac{\partial A_p}{\partial z} &= -\frac{1}{2} \alpha_{pl} A_p - \frac{1}{2} \alpha_{pFC} A_p - \frac{1}{2} \frac{\beta_{TPA}}{A_{p,eff}} |A_p|^2 A_p - \frac{\beta_{TPA}}{A_{p,eff}} |A_s|^2 A_p \quad (7) \\ &+ i \gamma_{p,p} |A_p|^2 A_p + i 2 \gamma_{p,s} |A_s|^2 A_p + i \frac{2\pi}{\lambda_p} \Delta n_{\lambda_p} A_p \end{aligned}$$

$$\begin{aligned} \frac{\partial A_s}{\partial z} &= -\frac{1}{2} \alpha_{sl} A_s - \frac{1}{2} \alpha_{sFC} A_s - \frac{1}{2} \frac{\beta_{TPA}}{A_{s,eff}} |A_s|^2 A_s - \frac{\beta_{TPA}}{A_{s,eff}} |A_p|^2 A_s \quad (8) \\ &+ i \gamma_{s,s} |A_s|^2 A_s + i 2 \gamma_{s,p} |A_p|^2 A_s + i \frac{2\pi}{\lambda_s} \Delta n_{\lambda_s} A_s \end{aligned}$$

To observe the dynamics evolutions of pulse along the SOI, above equations can be calculated numerically.

3. Numerical results

To observe easily the self-compression pulse in SOI waveguide, picosecond pulse is chosen in our modeling, whose dispersion length is further larger than the waveguide length of several millimeters or centimeters. Therefore, the nonlinear propagation equations of optical waves can be described by the Eqs. (7) and (8) that can be calculated by the well-known 4th Runge-kutta method.

In simulation, the shapes of pump and signal pulses can be expressed by

$$A(0, T) = \sqrt{P_{p0,s0}} \cdot \exp\left[-\frac{1}{2} \left(\frac{T}{T_{p0,s0}}\right)^{2m}\right] \quad (9)$$

where P_0 is the incident pulse peak power. T_0 is the half width at 1/e intensity point. m denotes the sharpness degree of pulse ($m=1$: Gaussian pulse, $m>1$: super-Gaussian pulse), in our simulations, the signal pulse has the waveform of Gaussian pulse, and the super-Gaussian pulse with $m=3$ is used as pump pulse, which can be obtained by the directly modulated semiconductor laser, and can make the outcome signal pulse to be more perfect.

According to the literatures [12, 17], the parameters for simulations are listed in Table 1.

Table 1. Simulation parameters.

Parameter	Definition	Value
n_2	Nonlinear coefficient	$6 \times 10^{-18} \text{ m}^2 \cdot \text{W}^{-1}$
α_l	Waveguide linear loss coefficient	$0.22 \text{ dB} \cdot \text{cm}^{-1}$
β_{TPA}	Two-photon absorption coefficient	$0.5 \text{ cm} \cdot \text{GW}^{-1}$
λ_p	Pump wavelength	1550 nm
λ_s	Signal wavelength	1310 nm
W	Rib waveguide width	900 nm
H	Rib height	780 nm
h	Slab height	390 nm
S, S'	Effective surface recombination velocity	$80 \text{ m} \cdot \text{s}^{-1}$
D	Diffusion coefficient	$16 \text{ cm}^2 \cdot \text{s}^{-1}$
c	Light velocity in vacuum	$2.99792458 \text{ m} \cdot \text{s}^{-1}$
\hbar	Reduced Planck constant	$1.06 \times 10^{-34} \text{ J} \cdot \text{s}$

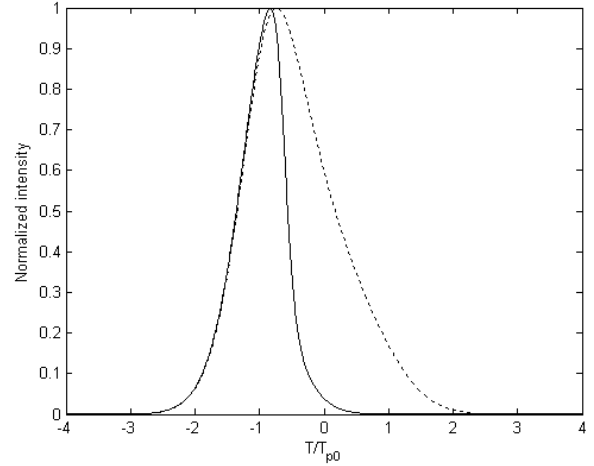
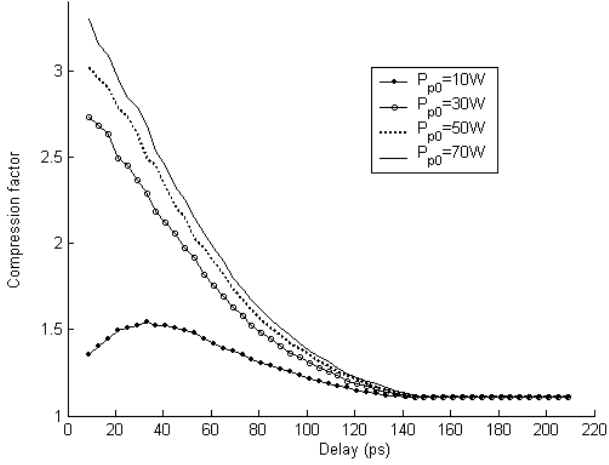


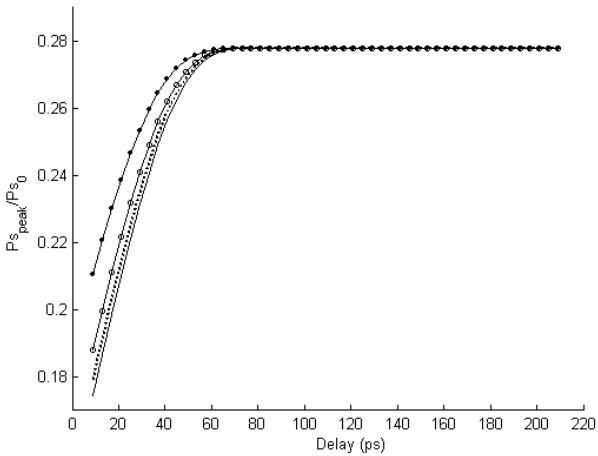
Fig. 2. The normalized output signal pulse at the end of 5-mm long waveguide (the dashed line: without pump pulse, the solid line: with pump pulse).

Fig. 2 illustrates, respectively, the normalized output signal waveforms at the end of 5-mm long waveguide with $P_{s0}=10 \text{ W}$ at the input for two cases of $P_{p0}=0$ and $P_{p0}=50 \text{ W}$. In calculations, both pump and signal pulse widths are $T_0=100 \text{ ps}$. The initial delay time, T_{d0} , of two pulses is equal to 50ps, where pump pulse lags the signal pulse with $T_{d0}>0$, on the contrary, which is ahead of signal pulse for $T_{d0}<0$. From the figure, it is clearly shown that while pump power is absent, the output signal waveform is distorted by the nonlinear response in SOI waveguide, i.e., the front end of pulse will shift forward due to TPA dominance, and the trailing edge has long duration time because of FCA dominance. However, the total pulse still exhibits the property of self-compression in duration time resulting that the pulsewidth, at full width of half maximum (FWHM), is compressed to $\sim 160 \text{ ps}$ comparing with the input FWHM of 166.5 ps. In reality, the self-compression pulse obtained need be compressed further to improve the signal quality. For comparison, the solid pulse profile shows the output waveform in the case of $P_{p0}=50 \text{ W}$ and $T_{d0}=50 \text{ ps}$ in the Fig. 2 where the trailing edge of outcome signal pulse is further suppressed while pump pulse is co-propagating in the waveguide. The behavior can be explained that when launch pump pulse suitably lags the signal pulse at the input end, the trailing edge of signal pulse will overlap with the high intensity pump pulse in time duration, whose energy will be absorbed by the process of non-degenerate TPA. As a consequence, the outcome pulsewidth can be shortened to $\sim 60 \text{ ps}$. It is worthy noting that the output leading edge holds on nearly unchanged comparing with the case of $P_{p0}=0$ because of having no cross nonlinear modulation between the pulses in the leading region of signal pulse. To obtain high quality output pulse, the initial delay time, T_{d0} , between a high intensity pump pulse and signal pulse must be positive. If it is large enough that both of pulses are separated completely in time region as a result of the outcome pulse that still keeps on the self-compression

waveform. In the system, the pump energy, the input pulsewidth, and total waveguide length will have prominent influences on the outcome, which will be discussed in detail in the following paragraphs.



(a)

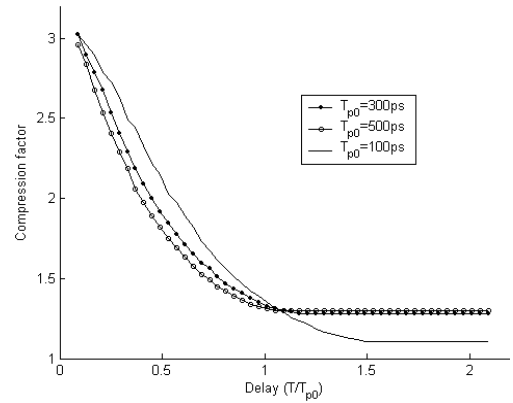


(b)

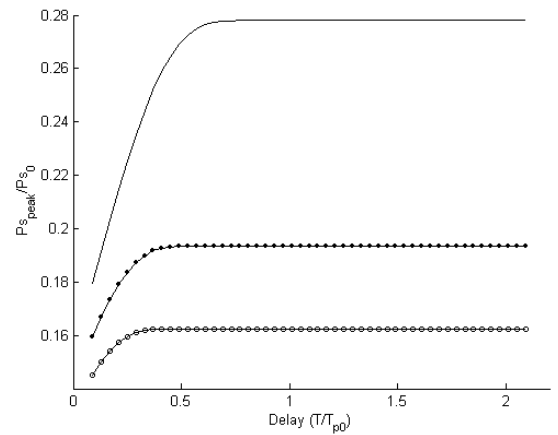
Fig. 3. The output pulse properties as a function of initial delay time between pump and signal pulses at the end of 5-mm long waveguide for different input pump peak powers with $T_{p0}=T_{s0}=100\text{ps}$. (a) Compression factor; (b). Peak power ratio.

In this paragraph, we will focus our attention on the change of output signal pulse with different delay times between the pump and signal pulses. Fig. 3 (a) and (b) demonstrate the compression factor (=input FWHM/output FWHM) and peak power ratio (=output peak power/input peak power) of output signal pulse as a function of initial delay time for four cases of $P_{p0}=10\text{W}$, 30W , 50W , and 70W , respectively. Other parameters are the same as Fig. 2. From the figure, the output pulse properties can be controlled by varying the initial delay time. After delay time arrives at $\sim 145\text{ps}$, the all of compression factors tend to a steady value. The phenomena imply that both pulses separate fully in time, i.e., no nonlinear interaction

between the two pulses occur. Another issue is that peak powers will also hold on steady after delay time of $\sim 60\text{ps}$. These various trends demonstrate that the peaks of two pulses are also separate during the propagation. When the pump pulse is overlapping with the trailing edge of signal pulse, signal pulse will be compressed by the non-degenerate TPA that is dependent strongly on the pump peak power under the condition of a fixed signal power, i.e., the compression factor will be increased with increasing the pump peak power in the case of having same delay time, which may be up to ~ 3 for $P_{p0}=70\text{W}$. The results are because more energy will be absorbed by the nonlinear process of non-degenerate TPA that will also become stronger when increasing the pump power. From the Fig. 3 (a), it isn't difficult to find that the compression will arrive at a steady state due to saturation depletion when having enough high power level for pump pulse. Notice that the output peak power is decreasing as increasing the pump peak power before the peaks of two pulses are separated, which will also get to be steady after saturation depletion, and is displayed in Fig. 3 (b).



(a)



(b)

Fig. 4. The output pulse properties as a function of initial delay time between pump and signal pulses at the end of 5-mm long waveguide for different pulsewidth with $P_{p0}=50\text{W}$, $P_{s0}=10\text{W}$. (a) Compression factor; (b) Peak power ratio.

On the other hand, when changing the pulse widths, the output outcome will also have variation, which can be seen in the Fig. 4 (a) and (b) where the compression factor and peak power ratio are shown for three cases of $T_{p0}=T_{s0}=100$ ps, 300 ps and 500 ps, respectively. It is clearly shown that when the input powers are fixed for two pulses, as extending the input pulsewidth, the output peak power will decay quickly because of the nonlinear losses including TPA and FCA increased. However, in these cases, the compression factors experience the course of contrary variation compared with the output peak power. Another remarkable issue is that pulse edges will become shaper with increasing the pulsewidth, as a consequence, the time of separation for both pump and signal pulses is equal to $\sim 1T_{p0}$ for $T_{p0}=T_{s0}=300$ ps, and 500 ps, which is increased to $\sim 1.5T_{p0}$ for input pulsewidth of 100ps.

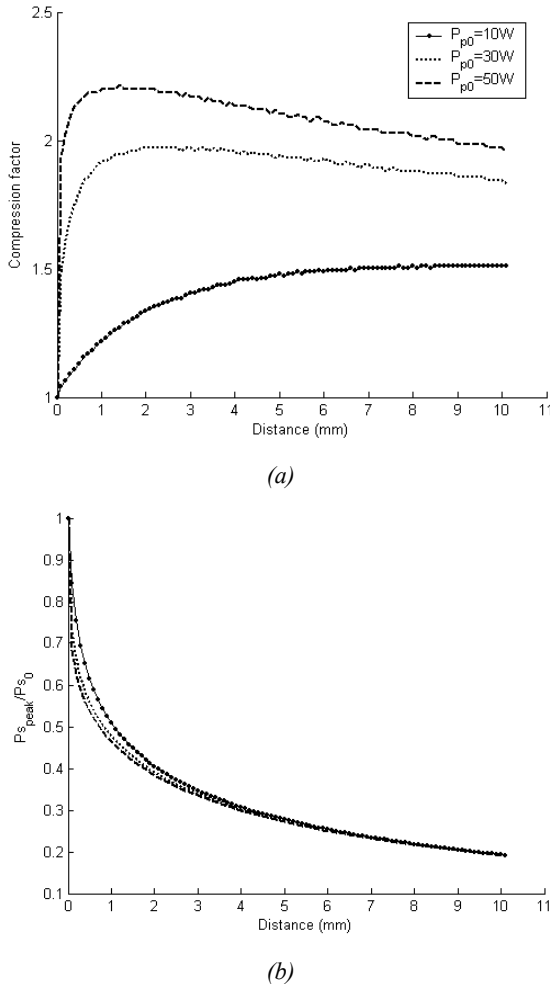


Fig. 5. The output pulse properties as a function of transmission distance for different launch pump powers with $T_{d0}=50$ ps, $T_{p0}=T_{s0}=100$ ps. (a). Compression factor, (b). Peak power ratio.

In the final paragraph, we will focus on the influence of waveguide length on the outcome. Fig. 5 (a) and (b) shows that the output signal pulse properties against the variation of waveguide length for different pump powers. We can see that the output peak will decrease sub-linearly

with increasing the waveguide length because the nonlinear interaction distance between pump and signal pulses and the influences of nonlinear and linear losses on the signal pulse are also increased. Nevertheless, after the propagation distance is up to ~ 5 mm, the output peak power is insensitive in the following propagation section with the variation of input pump power as a result of saturation depletion. Contrarily, the compression factors take on different output outcome for different pump power versus the waveguide length. For the cases of $P_{p0}=30$ W, and 50 W, the compress factors are increased to maximum at the ~ 1 mm long initial section of waveguide because of strong non-degenerate TPA between two pulses, which, however, can arrive at the maximum at ~ 10 mm long waveguide position due to the decreased nonlinear interaction as the input peak power is decreased to 10 W. In the subsequence, the pulsewidth will be broadened due to nonlinear process. Based on the above analysis, to achieve high quality pulse shaping, the high intensity pump pulse and appropriate waveguide length and the initial delay time should have well trade-off in the project proposed.

4. Conclusions

A technique for self-compression pulse shaping has been proposed and investigated by utilizing the nonlinear process of non-degenerate TPA between co-propagating pump and signal pulses in SOI optical waveguides, which is a feasible approach for pulsewidth reduction by simply adjusting the initial delay, and has potential applications in optical communications and switching. In this paper, we have presented the numerical results of pulse shaping with pulse duration up to one hundred of picosecond so that the dispersion and pulse walk-off are not taken into account, which, however, will produce significant influences on the pulse with femtosecond duration. So, another pulse shaping technique should be explored in our future research.

Acknowledgements

This work was supported by Chinese National Science Foundation (grant 60677023) and Chinese National High Technology Research and Development Program (grant 2006AA01Z240).

References

- [1] B. Jalali, S. Fathpour, J. Lightwave Technol. **24**, 4600 (2006).
- [2] H. S. Rong, R. Jones, A. S. Liu, O. Cohen, D. Hak, A. Fang, M. Paniccia, Nature **433**, 725 (2005).
- [3] H. S. Rong, A. S. Liu, R. Jones, O. Cohen, D. Hak, R. Nicolaescu, A. Fang, M. Paniccia, Nature **433**,

- 292 (2005)
- [4] A. S. Liu, H. S. Rong, R. Jones, O. Cohen, D. Hak, M. Paniccia, *J. Lightwave Technol.* **24**, 1440 (2006).
- [5] T. K. Liang, L. R. Nunes, T. Sakamoto, K. Sasagawa, T. Kawanishi, M. Tsuchiya, G. R. A. Priem, D. Van Thourhout, P. Dumon, R. Baets, H. K. Tsang, *Opt. Express* **13**, 7298 (2005).
- [6] L. Liao, A. Liu, D. Rubin, Basak J. Y. Chetrit, H. Nguyen, R. Cohen, N. Izhaky, and M. Paniccia, *Electron. Lett.* **43**, 1196 (2007)
- [7] M. A. Foster, A. C. Turner, R. Salem, M. Lipson, A. L. Gaeta, *Opt. Express* **15**, 12949 (2007).
- [8] Q. Fang, P. Chen, H. L. Xin, C. X. Wang, F. Li, Y. L. Liu, *Chin. Phys. Lett.* **22**, 1452 (2005).
- [9] S. J. Xiao, M. H. Khan, H. Shen, M. H. Qi, *J. Lightwave Technol.* **26**, 228 (2008).
- [10] J. W. Wu, F. G. Luo, Z. H. Yu, Q. Tao, *Optoelectron. Adv. Mat.-Rapid Comm.* **2**, 466 (2008).
- [11] J. M. Tang, K. A. Shore, *IEEE J. Quantum Electron.* **15**, 93 (1999).
- [12] D. Dimitropoulos, R. Jhaveri, R. Claps, J. C. S. Woo, B. Jalali, *Appl. Phys. Lett.* **86**, 07115 (2005).
- [13] V. M. N. Pasaro, F. de Leonardis, *Opt. and Quantum Electron.* **38**, 9 (2006).
- [14] V. M. N. Pasaro, F. De Leonardis, *J. Lightwave Technol.* **24**, 2920 (2006).
- [15] X. G. Chen, N. C. Chen, R. M. Osgood, *IEEE J. Quantum Electron.* **42**, 160 (2006).
- [16] R. Dekker, N. Usechak, M. Forst, A. Driessen, *J. Phys. D-Appl. Phys.* **40**, R249 (2007).
- [17] Q. Lin, J. D. Zhang, P. M. Fauchet, G. P. Agrawal, *Opt. Express* **14**, 4786 (2006).

*Corresponding author: jwwu@hhu.edu.cn